Contents lists available at ScienceDirect

Agricultural and Forest Meteorology

Hydraulic determinants of drought-induced tree mortality and changes in tree abundance between two tropical forests with different water availability

Yong-Qiang Wang [a], Hui-Qing Song [a], Ya-Jun Chen [b], Pei-Li Fu [b,c], Jiao-Lin Zhang [b], Kun-Fang Cao [a,*], Shi-Dan Zhu [a,*]

[a] State Key Laboratory for Conservation and Utilization of Subtropical Agro-bioresources, Guangxi Key Laboratory of Forest Ecology and Conservation, Guangxi University, Daxuedong Road 100, Nanning, Guangxi 530004, China
[b] CAS Key Laboratory of Tropical Forest Ecology, Xishuangbanna Tropical Botanical Garden, Chinese Academy of Sciences, Menglun, Mengla, Yunnan 666303, China
[c] Ailaoshan Station of Subtropical Forest Ecosystem Studies, Xishuangbanna Tropical Botanical Garden, Chinese Academy of Sciences, Jingdong, Yunnan 676209, China

ARTICLE INFO

ABSTRACT

Because of climate change, extreme droughts have become more frequent and caused widespread tree mortality, and thus significant shifts in community structure and function in many forests. Hydraulic failure is a major cause of drought-induced tree mortality. However, its effects on tree dynamics during repeated extreme droughts in tropical forests with different soil water availability are poorly understood. In this study, we surveyed the mortality rate and change in abundance (basal area) for 29 tree species from a humid tropical ravine rainforest (TRF) and an adjacent dry tropical karst forest (TKF) between 2004 and 2015. During this period, two extreme droughts occurred. We measured leaf and stem hydraulic-related traits and analyzed the trait–demography relationships. Our results showed that repeated extreme droughts induced an increase in tree mortality, and thus significantly affected the change of species abundance in the two forest communities. In both forests, the tree species with higher stem embolism resistance were more likely to survive extreme droughts, and increased in basal area during the census period. Moreover, the tree species in the two forests exhibited contrasting hydraulic strategies to deal with extreme drought. The lower mortality rate was associated with larger leaf and stem hydraulic safety margins in the TRF, but with more negative leaf hydraulic safety margin and stronger vulnerability segmentation (larger difference in embolism resistance between leaf and stem) in the TKF. This study expands our understanding of the hydraulic mechanisms to cope with extreme droughts in tropical tree species grown in different substrates under the present and future climatic conditions.

1. Introduction

Drought-induced tree mortality due to climate change, resulting in profound changes in community composition and ecosystem functions has been reported across moist-to-arid forests worldwide (Phillips et al., 2010; Choat et al., 2012; Anderegg et al., 2019; Bauman et al., 2022). The frequency of extreme droughts is increasing in the 21st century (Zhang et al., 2007; Dai, 2013; Cook et al., 2014); therefore, rendering the prediction of drought survival of forest tree species an important research topic (McDowell, 2011; Meir et al., 2015; Barros et al., 2019; Chen et al., 2021a). Hydraulic failure (substantial loss of hydraulic function in the xylem) is the principal mechanism underlying tree mortality in many forest ecosystems during periods of drought (McDowell, 2011; Anderegg et al., 2016; Choat et al., 2018; Brodribb et al., 2020; Nolan et al., 2021). Therefore, exploring the relationships between hydraulic traits and tree mortality rate provides an effective trait-based approach to forecasting forest responses to intensified droughts (Hammond et al., 2019; Powers et al., 2020; Pivovaroff et al., 2021).

Water potential at 50% loss of hydraulic conduction (P50), calculated from vulnerability curve, estimates the resistance to embolism and the threshold for hydraulic failure in leaves and stems (Anderegg et al., 2016; Chen et al., 2021a). The hydraulic safety margin (HSM), i.e., the difference between the minimum water potential experienced by a plant

---

* Corresponding authors.
E-mail addresses: kunfangcao@gxu.edu.cn (K.-F. Cao), zhushidan@gxu.edu.cn (S.-D. Zhu).

species in the field and P50, quantifies the degree of hydraulic risks under drought (McDowell, 2011; Delzon and Cochard, 2014) and can be expressed at the stem (HSM$_{stem}$; Choat et al., 2012; Mcculloh et al., 2015) and leaf levels (HSM$_{leaf}$; Bucci et al., 2013; Skelton et al., 2017). Previous studies from tropical and subtropical forests have revealed that the HSM is synergistic between the leaves and stems (Pivovaroff et al., 2018; Levionnois et al., 2020), and a larger HSM of either the leaves or stems indicates a lower risk of hydraulic failure and are thus associated with lower tree mortality due to drought (Rowland et al., 2015; Anderegg et al., 2016; Bauman et al., 2022). However, in other arid woodlands, smaller HSM$_{leaf}$ leads to a lower mortality rate (Creek et al., 2018; Zhang et al., 2019) because substantial loss of leaf hydraulic conductance can prevent further water loss of the main stem (Bucci et al., 2013; Pivovaroff et al., 2014; Tan et al., 2020). This refers to a hydraulic strategy termed vulnerability segmentation, defined as the difference between P50$_{leaf}$ and P50$_{stem}$ (P50$_{leaf-branch}$; Levionnois et al., 2020). Stronger vulnerability segmentation (larger values of P50$_{leaf-branch}$) indicates that the hydraulic functioning of stems that are metabolically more costly to produce can be preserved by sacrificing cheaper and more vulnerable leaves under droughts (Bucci et al., 2013; Pivovaroff et al., 2014). Thus, tree species from humid and arid environments are equipped with different hydraulic strategies and may represent contrasting hydraulic–mortality relationships.

Asian tropical forests are tropical biodiversity hotspots (Myers et al., 2000). Moreover, in southeastern Asia, large karst landscapes developed from soluble carbonate rocks and host forests with distinct species compositions and forest structures (Zhu et al., 2003; Geekiyanage et al., 2019; Li et al., 2021). Tropical forests on non-karst and karst soils can be found in the same region. Compared to the non-karst forest, karst forest habitats are characterized by widespread rock outcrops (Liu et al., 2014), thin soil layers, and leaking substrates, and therefore low soil water availability (Chen et al., 2015; Fu et al., 2019). Tree species growing on karst and non-karst substrates also exhibit different hydraulic characteristics and drought responses. Compared to the tree species of tropical non-karst forests, karst tree species experience significantly lower leaf water potential (Chen et al., 2015). However, they have higher sapwood density, smaller vessel diameter, and greater embolism resistance to adapt he dry karst environment (Zhu et al., 2017). Over the past several decades, climate change has resulted in increased frequency and intensity of extreme droughts in tropical China (Qiu, 2010; Qiao et al., 2021), which has proven to be the main driver of tree dynamics in Chinese tropical forests (Zhou et al., 2014). However, it is still uncertain whether the effects of increasing droughts on the mortality of tree species and their hydraulic determinants differ between tropical karst and non-karst forests.

Therefore, we investigated the mortality rate and changes in the stem basal area in two permanent 1 ha plots in a tropical ravine rainforest (non-karst) and an adjacent karst forest in southwestern China. We selected 29 tree species and conducted eight community censuses in the two forests from 2004 to 2015, during which two severe droughts occurred. Additionally, we measured the trees' leaf and stem vulnerability curves, minimum water potential, specific leaf area, and wood density. The main objective of this study was to characterize the trait–mortality relationships in the two forests. We hypothesized that: (1) a lower mortality rate and an increase in the basal area were associated with greater P50$_{stem}$ and larger HSM$_{stem}$ in both forests; and (2) leaf-to-stem vulnerability segmentation in the dry karst forest was stronger than that in the humid tropical ravine rainforest, and was a predictor of tree mortality in the karst forest.

2. Materials and methods

2.1. Study sites and plant materials

The present study was conducted in two permanent 1 ha (100 × 100 m) plots of primary tropical forests in the Xishuangbanna National Nature Reserve in southern Yunnan, China. Plot 1 was in the ravine sub-protective area (tropical ravine rainforest, TRF; 21°55′39″N, 101°15′55″E; 560 m a.s.l.), which was dominated by *Pometia pinnata, Barringtonia fusicarpa, Ardisia thyrsiflora*, and *Saprosma ternata*. The mean height of canopy trees can reach 30 m. The soil was laterite developed from the siliceous rock and with a depth of approximately 200 cm (Chen et al., 2015), with soil pH of 4.51, and N and P of 0.21% and 0.028%, respectively (Xia et al., 2016). Plot 2 was in the karst sub-protective area (tropical karst forest, TKF; 21°54′35″N, 101°16′52″E; 640 m a.s.l.), which was about 10 km away from Plot 1. This site is characterized by limestone rock outcrop (90% of the site), patchy calcareous soil, and rapid water leakage because of porous limestone rocks (Liu et al., 2014; Chen et al., 2015), as well as soil N and P deficiency (Zhang et al., 2015). Compared to TRF, this site has relatively high soil pH (6.62) and Ca and Mg content (Zhu et al., 2021). The dominant tree species were *Cleistanthus sumatranus, Celtis philippensis*, and *Lasiococca comberi*. The mean height of canopy trees can reach 21 m.

The study sites were strongly influenced by the tropical monsoon climate. According to the long-term climate data from the nearby meteorological station in the Xishuangbanna Tropical Botanical Garden (XTBG, Fig. 1), the mean annual precipitation and temperature are 1500 mm and 21.5 °C, respectively. The dry season lasts six months (November–April), with approximately 20% of the annual rainfall occurring during this period (Fig. S1). A recent study reported a significant tendency of warming and drying of the climate in this region, with a reduction in precipitation > 20 mm yr^{-1} during 2000–2016 (Qiao et al., 2021). In addition, two El Niño events occurred in 2004–2005 and 2009–2010 in the study site (Liu et al., 2021). The standardized precipitation evapotranspiration index (SPEI) was lower than −2 during those periods; such extreme droughts caused an increase in tree mortality in the forests (Fig. S1).

We investigated 18 and 11 tree species from the TRF and TKF, respectively. These tree species included both high- and low-abundances in each forest community (Table 1). All 18 tree species in the TRF were evergreen as the area is dominated by evergreen tree species. The TKF, located in a drought-prone area, includes a proportion of deciduous woody species (approximately 33%). Therefore, three of the 11 karst tree species were semi-deciduous, namely *Cipadessa baccifera, Croton crassifolius*, and *Mayodendron igneum*. They shed leaves in the mid-dry season and begin to flush new leaves in the late dry season. For each species, three to five individuals with a diameter at breast height (DBH) comparable to the mean DBH value of that species in the plot were sampled for trait measurements.

2.2. Community census, tree mortality, and changes of stem basal area

The two forest plots were established in 2004. In the initial inventory, all trees with a DBH ≥ 1 cm were tagged and identified, and their height and DBH were recorded. Subsequently, seven community censuses were conducted in the wet season in 2005, 2006, 2007, 2008, 2009, 2010, and 2015. During each census, the survival status of each tagged individual was recorded: dead standing trees (the trunk of a tree that was dead but did not fall), fallen dead wood, and living trees. The tree mortality was counted if it became standing dead or fallen dead during a census. The DBH and height of the living tagged individuals were measured, and recruits with DBH ≥ 1 cm were tagged and measured at each census.

For each studied tree species monitored from 2004 to 2015, we calculated the overall mortality rate (MR$_{2004-2015}$,%) using the following equation: MR$_{2004-2015}$ = 100 × (N$_{2004}$ − N$_{2015}$)/N$_{2004}$, where N$_{2004}$ is the initial individual number in 2004 and N$_{2015}$ is the number of survivors in 2015.

2.3. Measurements of stem and leaf traits

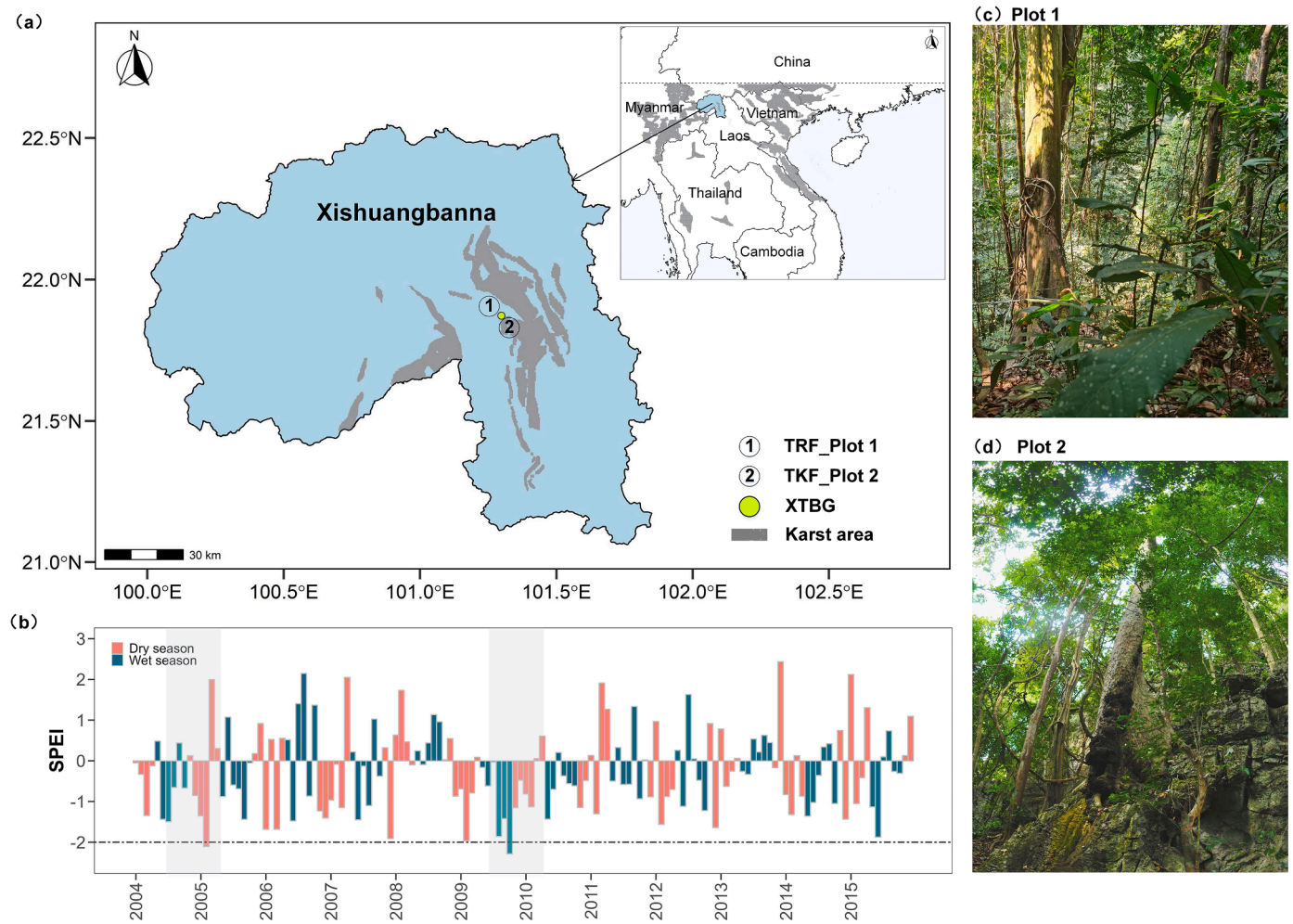The improved bench drying method was used to construct

Fig. 1. (a) Geographical location of the study region in Xishuangbanna, southwestern China, and the gray area represents the karst landform (Qiao et al., 2021). (b) Monthly changes of the standardized precipitation evapotranspiration index (SPEI) during 2004–2015. The SPEI can be calculated on a range of timescales from 1-month data (SPEI-1) of this region, downloaded from the Global SPEI database (https://spei.csic.es/map/maps.html#months=0#month=8#year=2022). The red and green bars indicate the dry and wet seasons, respectively. The gray background shows El Niño events. Extreme drought is characterized as SPEI <-2 (Wang et al., 2021). The photographs illustrate the tropical ravine rainforest (TRF_Plot 1, c) and tropical karst forest (TKF_Plot 2, d).

vulnerability curves of the stem xylem (Sperry et al., 1988; Wheeler et al., 2013). In the early dry season, 20–30 canopy branches (100–150 cm long) from five different individuals per species were sampled in the early morning using a retractable pruner (maximum length of 20 m). All sampled branches were enclosed in black plastic bags with a wet towel and immediately transported to the laboratory. The maximum vessel length (MVL) of each species was measured using the air infiltration method (Ziegler et al., 2019). The branches were then allowed to dehydrate to obtain different water potentials. During dehydration, the leaf water potential was measured regularly. Upon reaching the desired water potential, the entire branch was wrapped in a plastic bag for 1–2 h to equilibrate. The water potential of three leaves from the distal, middle, and basal parts of the branch was measured using a pressure chamber (PMS Instrument Company, Corvallis, OR, USA). We assumed the equilibrium of the water potential of the whole branch when the difference in values was less than 0.1 MPa. The mean of the three leaf water potential values was used as the xylem water potential (Ψ_x). We conducted a release-tension procedure to avoid excision artefacts when cutting segments under high xylem tension (Wheeler et al., 2013). Briefly, at MVL, the branches were cut off under water from the basal ends and bagged. The cut end was inserted into water for approximately 30 min to rehydrate and release xylem tension. Next, we obtained a segment with the length over MVL under water from the middle part of the branch for hydraulic measurements (the range of the stem diameter

was 5–10 mm for the 25 species). The targeted stem segment was connected to the tubing with filtered (0.2 μm) and degassed 20 mM KCl solution under 0.005 kPa hydrostatic pressure. The initial flow rate (J_i) was recorded using a digital liquid flow meter (Liqui-FlowL10; Bronkhorst High-Tech BV, Ruurlo, Netherlands) connected to the flow analysis programs FlowDDE and FlowPlot (Nolan et al., 2021). Then, the segment was flushed at 0.1 MPa for 0.5–1 h to determine the maximum flow rate (J_{max}). The percentage loss of hydraulic conductivity (PLC;%) was calculated as PLC $= 100 \times (J_{max} - J_i)/J_{max}$. Finally, based on a series of xylem water potential values and the corresponding PLC, the vulnerability curve for each species was fitted with a Weibull model using the fitplc function of the 'fitplc' package (Duursma and Choat, 2017) in R 4.1.1. The P50$_{branch}$ (water potential at 50% loss of hydraulic conductivity) was calculated from each species' vulnerability curves (Fig. S9). The P50$_{branch}$ values of four species (*Celtis philippensis, Lagerstroemia tomentosa, Pistacia weinmanniifolia*, and *Polyalthia cerasoides*) were collected from published papers (Tan et al., 2020; Chen et al., 2021a, 2021b), which were measured at the same site by using the same method. It should be noted that above hydraulic measurements were done at the beginning of the dry season (without extreme droughts), during which the predawn leaf water was rather high (> -0.5 MPa; Zhu, unpublished data). Therefore, native xylem embolism could be minimal.

The rehydration kinetics method was used to establish the leaf hydraulic vulnerability curves (Brodribb and Holbrook, 2003; Wheeler

Table 1

The 29 tree species used in this study. Stem basal area is calculated as the sum of the cross-sectional areas at breast height of all individuals for that tree species in the 1-ha plot. # denotes semi-deciduous species.

Species	Family	Code	Basal area (cm^2 ha^{-1})	Mean DBH (cm)
Tropical ravine rainforest				
Pometia pinnata	Sapindaceae	Pop	70,661.49	23.01
Barringtonia fusicarpa	Lecythidaceae	Baf	25,648.55	14.59
Orophea laui	Annonaceae	Orl	6093.09	5.54
Saprosma ternata	Rubiaceae	Sat	1152.14	3.54
Baccaurea ramiflora	Euphorbiaceae	Bar	2446.9	5.98
Walsura robusta	Meliaceae	War	3079.86	6.67
Cleidion brevipetiolatum	Euphorbiaceae	Clb	3315.24	7.84
Drypetes indica	Euphorbiaceae	Dri	2630.98	4.47
Pseuduvaria trimera	Annonaceae	Pst	2191.6	5.91
Phoebe lanceolata	Lauraceae	Phl	596.63	4.3
Polyalthia simiarum	Annonaceae	Pos	820.18	4.54
Syzygium megacarpum	Myrtaceae	Sym	200.8	3.48
Acronychia pedunculata	Rutaceae	Acp	391.34	4.42
Beilschmiedia purpurascens	Lauraceae	Bep	1593.33	17.73
Syzygium cumini	Myrtaceae	Syc	172.95	4.25
Pygeum topengii	Rosaceae	Pyt	1331.02	19.33
Lasianthus sikkimensis	Rubiaceae	Las	81.84	3.11
Cinnamomum contractum	Lauraceae	Cic	113.03	4.94
Tropical karst forest				
Cleistanthus sumatranus	Euphorbiaceae	Cls	32,862.75	7.05
Celtis philippensis	Ulmaceae	Cep	6417.98	6.92
Lasiococca comberi	Euphorbiaceae	Lac	3785.4	5.95
Lagerstroemia tomentosa	Lythraceae	Lat	5476.32	35.03
Trigonostemon bonianus	Euphorbiaceae	Trb	703.22	3.9
Pistacia weinmanniifolia	Anacardiaceae	Piw	845.71	22.49
Cipadessa baccifera#	Meliaceae	Cib	446	12.77
Mitrephora calcarea	Annonaceae	Mic	153.26	7.68
Croton crassifolius#	Euphorbiaceae	Crc	432.98	16.57
Mayodendron igneum#	Bignoniaceae	Mai	697.92	10.13
Polyalthia cerasoides	Annonaceae	Poc	17.24	3.28

et al., 2013). The sampling and dehydration procedures were similar to those used for stem vulnerability curve measurements. Before determining the leaf hydraulic conductance (K_{leaf}), leaf-bearing branches were enclosed in a black bag for approximately 1 h to ensure that all the attached leaves had similar water potential (the difference between two leaves from the apical and basal parts of the same branch was less than 0.1 MPa). After measuring the initial water potential of equilibrated leaves (Ψ_0), a neighboring leaf was cut underwater, and the cut end was immersed for 10–300 s (t) to rehydrate the leaf to a rehydrated water potential, which was about half of the initial water potential of a given measurement. The rehydration duration (t) depended on the species and the level of leaf dehydration. Leaf hydraulic conductance was calculated using the equation $K_{leaf} = (C_{leaf}/t) \times \ln(\Psi_0/\Psi_f)$, where C_{leaf} is leaf capacitance. Leaf capacitance was calculated as: $C_{leaf} = \Delta RWC/\Delta\Psi \times (DM/LA) \times (WM/DM)/M$, where DM (g) is leaf dry mass, LA (cm^2) is leaf area, WM (g) is mass of leaf water at 100% relative leaf water content, and M is the molar mass of water (g mol^{-1}). $\Delta RWC/\Delta\Psi$ before leaf turgor loss point (TLP) was calculated from the leaf pressure–volume (P-V) relations (Tyree and Hammel, 1972; Johnson et al., 2018). The leaf P-V relations were determined by periodically measuring leaf mass (with a precision of 0.0001 g) and leaf water potential during dehydration under laboratory conditions and were analyzed using a P-V curve analysis program (Johnson et al., 2018). We calculated K_{leaf} at different Ψ_0 as described above, and constructed leaf vulnerability

curves by plotting K_{leaf} against Ψ_0 using a three-parameter sigmoid model in SigmaPlot 12.5 (Systat Software Inc., San Jose, CA, USA). P50$_{leaf}$ was used to estimate the vulnerability of leaves to hydraulic dysfunction (Levionnois et al., 2020). In this study, we measured P50$_{leaf}$ for 17 of the 29 tree species and obtained P50$_{leaf}$ of another nine tree species from our previous studies using the same method (Tan et al., 2020; Chen et al., 2021a, 2021b; Table S1). However, the P50$_{leaf}$ values of three species (*Orophea laui, Saprosma ternata*, and *Trigonostemon bonianus*) were not determined and thus were not included in the analysis.

The midday leaf water potential of the studied tree species in the two plots was measured in the peak drought in each year with extreme drought between 2007 and 2011 (Fu et al., 2012; Chen et al., 2015; Tan et al., 2020) and used as the minimum leaf water potential (Ψ_{min}) in this study. The branch HSM was calculated as HSM$_{branch}$ = Ψ_{min} – P50$_{branch}$ (Choat et al., 2012). The leaf HSM was calculated as HSM$_{leaf}$ = Ψ_{min} – P50$_{leaf}$ (Skelton et al., 2017). The leaf-stem hydraulic vulnerability segmentation was calculated as: P50$_{leaf-branch}$ = P50$_{leaf}$ – P50$_{branch}$ (Bucci et al., 2013).

Once hydraulic measurements of branches were finished, five branch segments were subsequently used for measuring wood density. We cut off a short segment (5 cm) from each branch, split it using a knife to remove pith and bark then determined the volume of the wood sample using the water displacement method (Perez-Harguindeguy et al., 2016). The sample was oven-dried at 70 °C for 48 h to obtain its dry mass. Sapwood density (WD, g cm^{-3}) was determined by dividing the dry mass by the volume of the sample. For each species, 20–30 leaves were sampled from each individual. The leaf area was measured using a leaf area meter (Li-3000A; LiCor, Lincoln, NE, USA), and the leaves were then oven-dried at 70 °C for 72 h to obtain the dry mass. Specific leaf area (SLA, cm^2 g^{-1}) was calculated as the ratio of leaf area to leaf dry mass.

2.4. Statistical analysis

To clarify the impact of tree size on the drought-induced mortality rate, we performed a logistic regression analysis with mortality rate as a binary response variable (0 = alive in 2015, 1 = died in 2015) to tree size (DBH) for all trees in each plot (Fig. S2; Powers et al., 2020). At the plot level, we investigated the role of tree diameter in determining mortality patterns by using individual trees' DBH size (stems $\geq$ 1 cm DBH), and the model did not include species as an effect. Furthermore, to better understand whether mortality risk and its dependence on size varied among species from 2004 to 2015, we conducted species-specific logistic regressions between DBH and mortality rate for 15 studied species with more than 30 individuals (stems $\geq$ 1 cm DBH).

We used an independent-samples *t*-test to compare the differences in traits between the two forest communities. The relationship between mortality rate and P50$_{branch}$, HSM$_{leaf}$, and P50$_{leaf-branch}$ in each plot was analyzed using weighted least-square linear or non-linear regression (exponential model with a better model fit, Table S2), with the number of individuals of each species in the plot as the weight, because mortality estimates are higher for species with more individuals (Powers et al., 2020).

We analyzed the change in basal area for each studied species following the methods described in previous studies (Soudzilovskaia et al., 2013; Li et al., 2015). Stem basal area is calculated as the sum of the cross-sectional areas at breast height of all individuals for that tree species in the 1-ha plot. The change in the basal area considers both the growth and mortality of tree species and is thus a more comprehensive indicator that can reflect the overall fitness status in the plant community (Iverson and Prasad, 1998; Ehrlén and Morris, 2015). The basal area was standardized using the following equation: $Z_i = (x_i - \bar{x})/\sigma_x$, where Z_i is the standardized basal area, x_i is the species' basal area in year i, $\bar{x}$ is the mean species' basal area of the eight community censuses, and σ_x is the standard deviation of the species' basal area. We then used

simple linear regression to examine the response of abundance to the year. The regression slope coefficient is referred to as the "basal area–year slope," and indicates the temporal trend of the species' basal area. The variation of the regression coefficients was named CV, which reflects the confidence boundaries of the relationships. Significant positive or negative regression slopes with ($P < 0.05$) indicate that species increased or decreased in abundance during 2004–2015. Non-significant regression slopes ($P > 0.05$) implied that the species abundance remained unchanged (Fig. S3; Table S1). The weighted regression analysis was used to explore the relationship between basal area-year slopes and hydraulic traits, with the inverse of CV as the weight, because species with more significant abundance–year relationships have larger weights in the analysis.

All analyses were performed in R 4.1.1 statistical software (The R Foundation for Statistical Computing) using packages "ggplot2" (Wickham, 2016), "Hmisc" (Harrell Jr, 2022), "lme4" (Bates et al., 2015), and "car" (Fox and Weisberg, 2019).

3. Results

3.1. Tree mortality in the two tropical forest communities

At the community level, tree mortality increased significantly with SPEI in the dry season in the two forests (Fig. S1b). The 29 tree species showed substantial interspecific differences in mortality rates during the whole census period (2004–2015). In the TRF, *Pygeum topengii, Lasianthus sikkimensis*, and *Beilschmiedia purpurascens* showed high mortality rates at 67%, 60%, and 50%, respectively. In the TKF, three semi-deciduous species (*Cipadessa baccifera, Croton crassifolius* and *Mayodendron igneum*) showed high mortality rate at 100%, 50% and 20%, respectively. Other TKF tree species showed mortality rates of less than 20% (Fig. 2).

At the community-level, tree DBH had a significant effect on mortality in the TRF and marginally significant effect in the TKF (Fig. S2). Small tree (DBH < 5 cm) with higher mortality rates (12.79% and 8.52%, respectively) in TRF and TKF, are more susceptible to drought-induced death than large trees (DBH > 20 cm; mortality rates, 0.82% and 0.37%, respectively). At the species level, only one species (*Lasiococca comberi*) out of the 15 tree species in this study (≥30 individuals) had significant relationships between DBH and the probability of tree mortality ($P < 0.05$; Fig. S2). And three species with more dead individuals in larger diameter classes, *Barringtonia fusicarpa* and *Pometia pinnata* in TRF, and *Cleistanthus sumatranus* in TKF (Fig. S2).

3.2. The differences in traits between the two forest tree species

On average, the TRF tree species exhibited significantly greater HSM_{leaf} and HSM_{branch} and less negative Ψ_{min} values than those in the TKF (Figs. 3 and S5). However, the mean values of $P50_{branch}$, $P50_{leaf}$, SLA, and WD did not differ significantly between the two forests (Figs. 3 and S5). The studied species showed a large interspecific variation in the $P50_{leaf-branch}$ (Fig. 3), and all the species had positive values of $P50_{leaf-branch}$ (i.e., $P50_{branch}$ was more negative than $P50_{leaf}$). However, there was no significant difference in the mean $P50_{leaf-branch}$ values between the two forests.

3.3. Relationships of stem and leaf traits to mortality rate and abundance change

In both TRF and TKF, $P50_{branch}$ was negatively correlated with mortality rate and positively correlated with the basal area–year slope, and $P50_{leaf-branch}$ was positively related to the basal area–year slope (Fig. 4). In the TRF, there were positive relationships between $P50_{leaf}$ and $P50_{branch}$ and between HSM_{leaf} and HSM_{branch} (Fig. S7). It was found that HSM_{leaf} was negatively related to mortality rate and positively related to the basal area–year slope, and that $P50_{leaf-branch}$ was not related to mortality rate (Fig. 4a–f, Table S2). By contrast, a lack of correlation between hydraulic safety of leaves and branches in the TKF (Fig. S7) and HSM_{leaf} was positively correlated with mortality rate and negatively with basal area–year slope (Fig. 4h, k). In addition, $P50_{leaf-branch}$ was negatively correlated with mortality rate (Fig. 4i). However, the mortality rate was not correlated with plant economic traits (e.g., SLA and WD) in either forest community (Fig. S8).

4. Discussion

Our results showed that tree mortality increased significantly at both community- and species-levels after extreme drought events in the two forests. Hydraulic traits rather than economic traits predicted the mortality rates. In both forests, tree species with higher xylem embolism resistance had lower mortality rates and substantially increased stem basal area after repeated extreme droughts. In addition, lower mortality
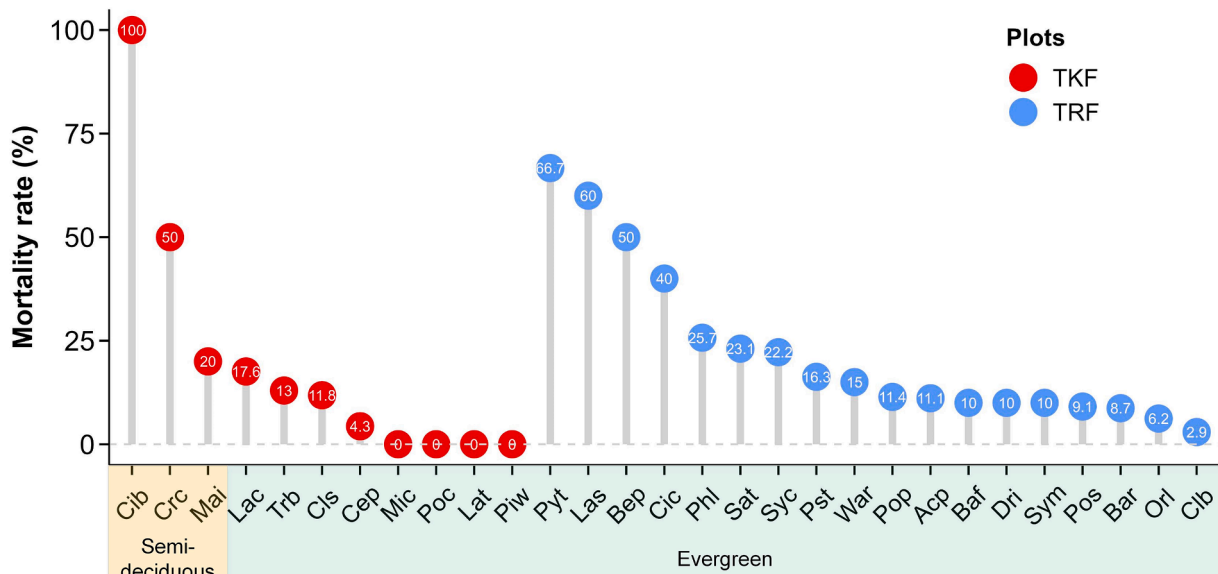

Fig. 2. Mortality rate of 29 tree species in the tropical ravine rainforest (TRF; blue circles) and tropical karst forest (TKF; red circles). Mortality rate is the percentage of tree mortality during 2004–2015. The species abbreviations are shown in the Table 1.
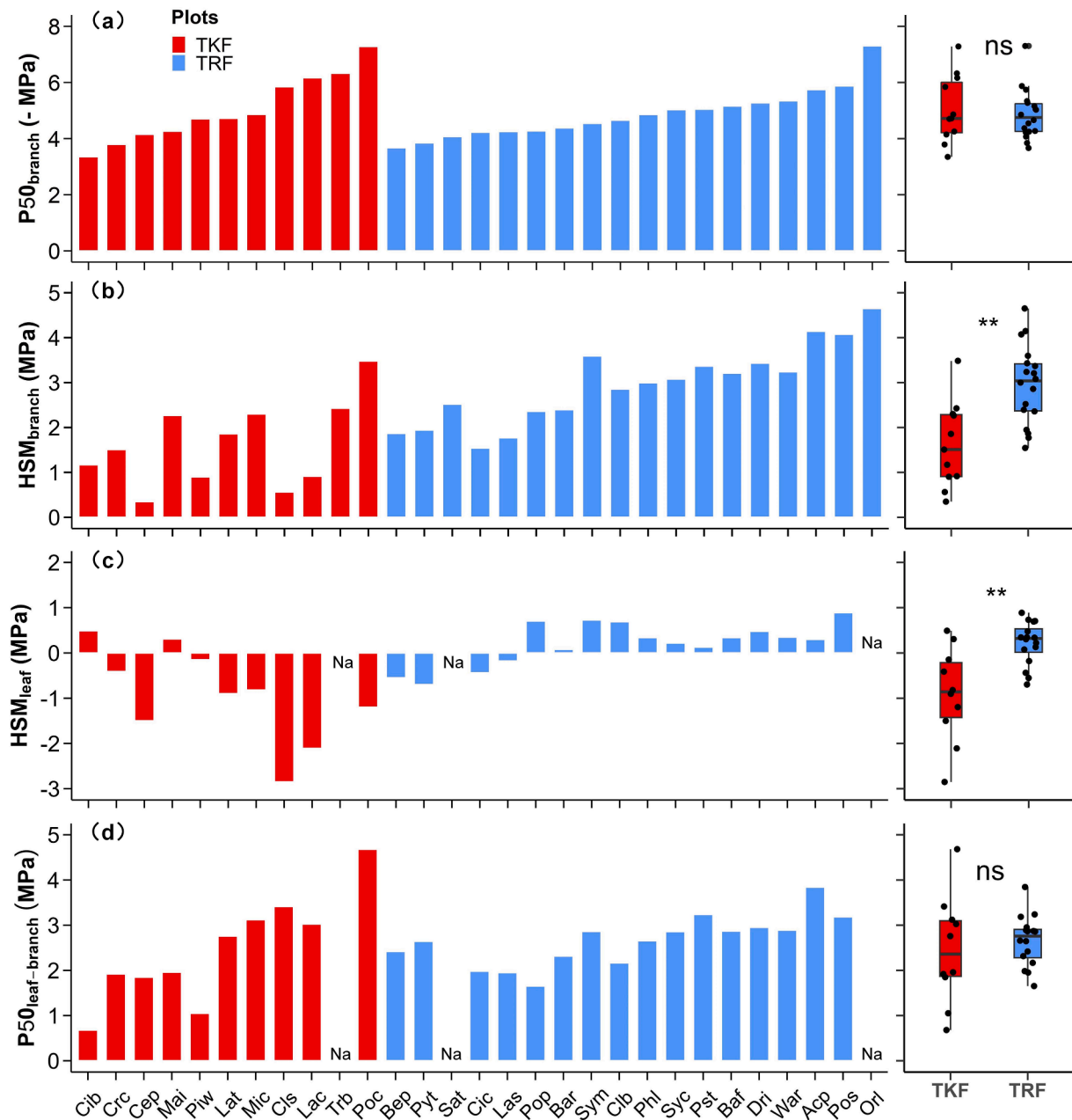
Fig. 3. Mean hydraulic traits of 29 tree species from the tropical ravine rainforest (blue bars) and tropical karst forest (red bars), respectively. $P50_{branch}$, water potential at 50% loss of hydraulic conductivity; HSM_{leaf}, leaf hydraulic safety margin; HSM_{branch}, branch hydraulic safety margin; $P50_{leaf-branch}$, leaf-stem hydraulic vulnerability segmentation. Traits are compared between TRF and TKF as two groups using t-tests (right panels). ** indicates significant difference at $P < 0.01$, ns indicates not significant. The abbreviations for the species names are defined in the Table 1. Na indicates data not available.

rates were associated with larger HSM_{leaf} and HSM_{branch} in TRF, but with smaller HSM_{leaf} and stronger vulnerability segmentation in TKF. This implies that TRF and TKF tree species exhibited different hydraulic strategies for coping with extreme droughts.

4.1. High xylem embolism resistance was related to low tree mortality and increased basal area after repeated extreme droughts in both forests

We found that tree species with lower $P50_{branch}$ were more likely to survive extreme droughts in both tropical forests (Fig. 4), which was consistent with other studies from tropical rain forests in the eastern Amazon (Rowland et al., 2015), *Eucalyptus* forests in eastern Australia (Brodribb et al., 2020; Nolan et al., 2021), and cross-species patterns of drought-induced tree mortality across the globe (Anderegg et al., 2016).

This is because high xylem embolism resistance could be an adaptation to extreme drought by reducing the possibility of hydraulic dysfunction. For example, although the dominant tree species (e.g., *Cleistanthus sumatranus* and *Lasiococca comberi*) in the karst forest experienced very low leaf water potential (−5.28 and −5.25 MPa) during extreme droughts, they had relatively low mortality rates owing to the wide hydraulic safety threshold that prevented hydraulic failure of the xylem ($P50_{branch}$ = −5.84 and −6.17, respectively; Fig. 3, Table S1). In addition, with the increasing of xylem hydraulic vulnerability, the mortality rate increased exponentially in the two forests (Fig. 4). This supports the fact that the number of the tree deaths dramatically increase when drought exceeds the hydraulic safety threshold of tree species in natural forests (Allen et al., 2015; Senf et al., 2020).

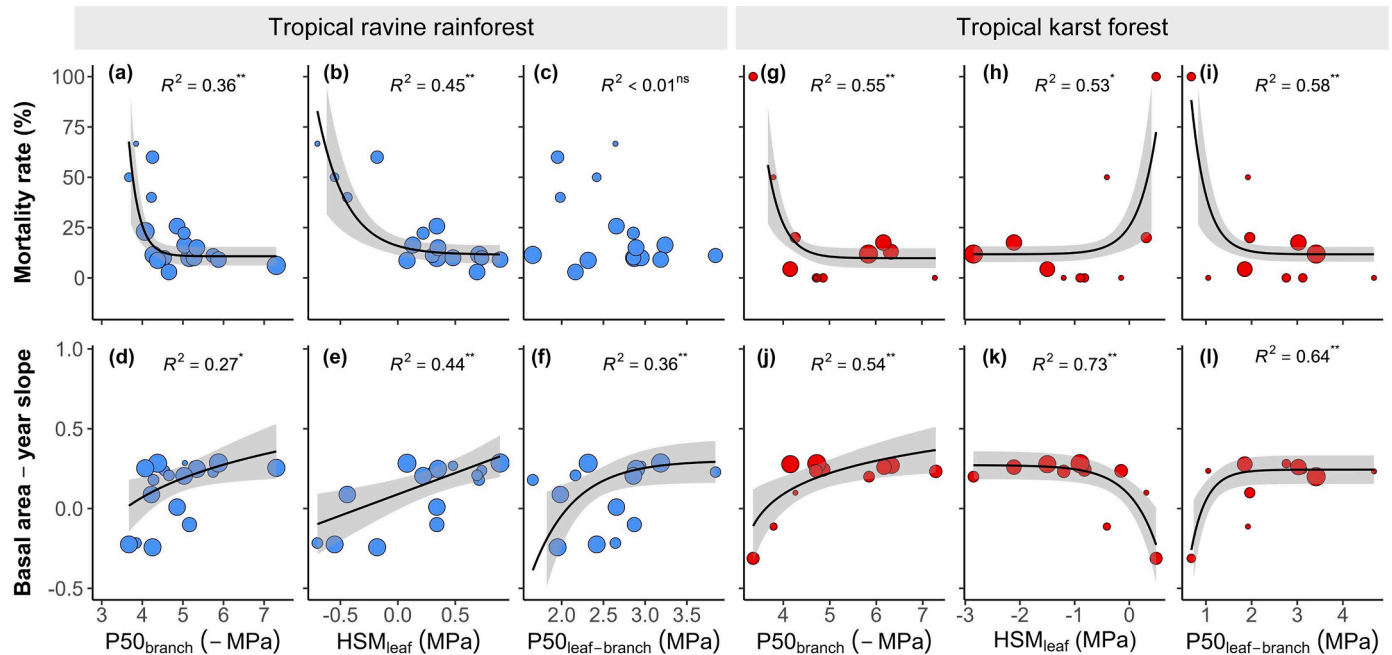Our results show that tree species with lower $P50_{branch}$ significantly

Fig. 4. Relationships between hydraulic traits and mortality rate, and basal area changes in the tropical ravine rainforest (blue dots: a-f) and tropical karst forest (red dots: g-l), respectively. Mortality rate is the percentage of tree mortality during 2004–2015. Point sizes are in accordance with the number of individuals for each species in the plot. Traits abbreviations are shown in Fig. 3. Black lines represent regressions and the gray areas represent the regression 95% confidence intervals. * and ** indicate significant difference at $P < 0.05$ and $P < 0.01$, respectively.

increased their stem basal area in the two tropical forests during the census period (Fig. 4), indicating that this hydraulic trait could further forecast community dynamics of tropical forests. This may be because changes of basal area were mainly caused by drought-induced tree mortality (Fig. S4c). Despite there not being a significant relationship between basal area-year slope and tree growth and recruitment rates (Fig. S4 b–d), we did not exclude these two factors that influence changes in basal area. Thus, future studies should include comprehensive analyses of the relationships between hydraulic traits and demography rates including growth, mortality, and recruitment (He et al., 2022). In additional, we did not record other potential disturbances causing tree death besides drought (e.g., insect attacks) during community-survey period and detect the influence of species interaction.

The two tropical forests differed markedly in water availability, with lower soil and leaf water potential during drought periods in the TKF than those in the TRF and (Chen et al., 2015; Fig. S5). Nevertheless, the TKF and TRF tree species showed similar average $P50_{branch}$ values (Fig. 3). This is in contrast with previous findings that TKF tree species are more resistant to embolism than TRF tree species (Chen et al., 2015; Zhu et al., 2017). Moreover, our results showed that the $P50_{branch}$ values in the present study assessed with the improved bench drying method were more negative than those in a previous study on the same tropical tree species assessed by the air-injection method (Zhu et al., 2017). It was established that the air-injection method could overestimate the vulnerability of the xylem to embolism in tropical tree species with long vessels (Chen et al., 2021b). Therefore, we recommend caution while using published data on xylem hydraulic safety because even trees in tropical moist forests may have fairly high xylem resistance to embolism.

4.2. Low mortality is associated with strong vulnerability segmentation in the dry tropical karst forest

In the TKF, we found that tree species with more negative HSM_{leaf} had lower mortality rates (Figs. 2 and 3). In a previous study in the same forest, Tan et al. (2020) found that the dominant canopy evergreen tree

species, such as *Celtis philippensis, Lasiococca comberi*, and *Cleistanthus sumatranus*, showed more negative HSM_{leaf} (−1.5 MPa, −2.11 MPa, and −2.85 MPa, respectively) under extreme droughts, consistent with their extensive terminal dieback. However, these dominant tree species showed a very low mortality rate (Fig. 2) based on the community census conducted in this study. This is because the substantial loss of leaf hydraulic conductance is an adaptive response to extreme droughts that prevents water loss and protects the main stems, consistent with the concept of vulnerability segmentation (Tyree and Ewers, 1991; Levionnois et al., 2020). Indeed, a negative relationship between HSM_{leaf} and $P50_{leaf-branch}$ was reported in this study (Fig. S7). Furthermore, stronger vulnerability segmentation was found to be significantly associated with lower tree mortality in the TKF (Fig. 4). These results support that species from arid habitats have developed strong leaf-to-stem vulnerability segmentation as a drought survival mechanism (Bucci et al., 2013; Zhang et al., 2019).

A proportion of deciduous tree species occur in tropical seasonally dry forests as an adaptation to low soil moisture availability (Zhu et al., 2003; Dahlin et al., 2017). A previous study demonstrated that deciduous tree species would become more abundant in tropical dry forests under climate change (Aguirre Gutiérrez et al., 2019). However, the two semi-deciduous species (*Cipadessa baccifera* and *Croton crassifolius*) in the TKF had a high mortality rate (100% and 50%, respectively). Similarly, Chen et al. (2021a) reported higher branch dieback and top-kill in semi-deciduous species than that in co-occurring evergreen species in a tropical savanna vegetation during an extreme drought. The authors inferred that this was because the water consumption through transpiration in semi-deciduous species continued during the late drought period, thus causing their water potential to cross the threshold of hydraulic failure (Chen et al., 2021a). Additionally, our results indicated that the two semi-deciduous species were less embolism-resistant than the evergreen, lacked vulnerability segmentation (Figs. 3 and S7), and were consequently susceptible to hydraulic dysfunction. It's worth noting that the species number is limited for species-rich tropical forests. For example, 11 species were used in the TKF, and the trait-mortality relationships are significantly driven by the two semi-deciduous species. In the future, more species will need to be selected to verify such

relationships.

4.3. Low mortality is associated with large leaf and stem HSM in the tropical ravine rainforest

On average, the 18 TRF tree species showed larger HSM_{leaf} and HSM_{branch} values than the TKF species (Fig. 3). Additionally, a larger HSM was associated with a lower mortality rate in the TRF (Fig. 4). Similarly, a correlation between HSM_{leaf} and mortality was also reported in a tropical seasonal rainforest (Powers et al., 2020). In tropical rain forests, some studies have indicated that more isohydric species had a larger HSM_{leaf} (Klein et al., 2014; Levionnois et al., 2021), as the result of stronger stomatal regulation to maintain leaf water potential above the hydraulic failure threshold of the leaves and stems (Liu et al., 2015; Pivovaroff et al., 2018; Creek et al., 2019), or because of access to underground water by deep root systems (Chitra Tarak et al., 2021). In a previous study at the same site, Chen et al. (2015) found the TRF tree species can maintain relatively high Ψ_{mid} during extreme droughts (mean value of -2.05 MPa) by lowering stomatal conductance by 82% and accessing deep soil water. However, whether other hydraulic strategies, such as high stem hydraulic capacitance to constrain transpiration-induced fluctuations in xylem tension (e.g., Meinzer et al. 2009) and leaf water uptake with leaf-wetting events (e.g., Eller et al. 2016) play a role in maintaining hydraulic balance, deserves further investigations.

4.4. Effect of tree size on mortality

We found the influence of tree size on drought-induced mortality in the analysis of the hydraulic trait-mortality relationship in both forests. At the forest level, small tree (DBH < 5 cm) with higher mortality rates in TRF and TKF, are more susceptible to drought-induced death than large trees (DBH > 20 cm), because the smaller trees have shallower root systems compared to the large individuals (Martínez-Garza et al., 2013; Uriarte et al., 2016; Trugman et al., 2018; Britton et al., 2022). This observation is consistent with other studies (Enquist and Enquist, 2011; Nolan et al., 2021; Britton et al., 2022). However, other studies have shown larger trees are more vulnerable (Bennett et al., 2015; Fettig et al., 2019), which may be because soil moisture deficit exceeds the water compensation of deep roots of the large tree exposed to droughts of greater duration. Thus, larger individual with higher water consumption become more vulnerable to drought (Trugman et al., 2018; Fettig et al., 2019). Therefore, studies considering intra-specific variations in hydraulic traits and DBH classes (e.g., Bittencourt et al. 2020, Gutierrez Lopez et al. 2021) are more valuable to address this question.

5. Conclusions

In both tropical forest communities of the present study, tree species with higher xylem embolism resistance had a low mortality rate and increased stand abundance after repeated extreme droughts, which is thus a good predictor of tree dynamics in the present and future environments regardless of habitat water regimes. In addition, the two forests tree species exhibited different hydraulic strategies to survive extreme droughts. Lower tree mortality was associated with higher leaf and stem HSMs in the tropical ravine rain forests with sufficient soil moisture and stronger leaf-to-stem vulnerability segmentation in the dry tropical karst forest. We also recommend testing the hydraulic traits-tree dynamics relationships found in this study in a large range of forest communities.

Supporting information

Additional supporting information on this study has been uploaded with the submission.

CRediT authorship contribution statement

Yong-Qiang Wang: Writing – original draft, Formal analysis, Data curation, Writing – review & editing. **Hui-Qing Song:** Formal analysis, Data curation, Writing – review & editing. **Ya-Jun Chen:** Resources, Writing – review & editing. **Pei-Li Fu:** Resources, Writing – review & editing. **Jiao-Lin Zhang:** Formal analysis, Data curation, Writing – review & editing. **Kun-Fang Cao:** Visualization, Formal analysis, Data curation, Writing – review & editing. **Shi-Dan Zhu:** Visualization, Writing – original draft, Resources, Writing – review & editing.

Declaration of Competing Interest

The authors declare that they have no known competing financial interests or personal relationships that could have appeared to influence the work reported in this paper.

Data availability

Data will be made available on request.

Acknowledgements

Supplementary materials

Supplementary material associated with this article can be found, in the online version, at doi:10.1016/j.agrformet.2023.109329.

References

Aguirre Gutiérrez, J., Oliveras, I., Rifai, S., Fauset, S., Adu Bredu, S., Affum Baffoe, K., et al., 2019. Drier tropical forests are susceptible to functional changes in response to a long-term drought. Ecol. Lett. 22 (5), 855–865. https://doi.org/10.1111/ele.13243.

Allen, C.D., Breshears, D.D., McDowell, N.G., 2015. On underestimation of global vulnerability to tree mortality and forest die-off from hotter drought in the anthropocene. Ecosphere 6 (8), t129. https://doi.org/10.1890/ES15-00203.1.

Anderegg, W.R.L., Anderegg, L.D.L., Kerr, K.L., Trugman, A.T., 2019. Widespread drought-induced tree mortality at dry range edges indicates that climate stress exceeds species' compensating mechanisms. Glob. Chang. Biol. 25 (11), 3793–3802. https://doi.org/10.1111/gcb.14771.

Anderegg, W.R.L., Klein, T., Bartlett, M., Sack, L., Pellegrini, A.F.A., Choat, B., et al., 2016. Meta-analysis reveals that hydraulic traits explain cross-species patterns of drought-induced tree mortality across the globe. Proc. Natl. Acad. Sci. 113 (18), 5024–5029. https://doi.org/10.1073/pnas.1525678113.

Barros, F.D.V., Bittencourt, P.R.L., Brum, M., Restrepo-Coupe, N., Pereira, L., Teodoro, G. S., et al., 2019. Hydraulic traits explain differential responses of Amazonian forests to the 2015 El Nino-induced drought. New Phytol. 223 (3), 1253–1266. https://doi.org/10.1111/nph.15909.

Bates, D., Maechler, M., Bolker, B.M., Walker, S.C., 2015. Fitting linear mixed-effects models using lme4. J. Stat. Softw. 67 (1), 1–48. https://doi.org/10.18637/jss.v067.i01.

Bauman, D., Fortunel, C., Delhaye, G., Malhi, Y., Cernusak, L.A., Bentley, L.P., et al., 2022. Tropical tree mortality has increased with rising atmospheric water stress. Nature. https://doi.org/10.1038/s41586-022-04737-7. Published online: 18 May 2022.

Bennett, A.C., McDowell, N.G., Allen, C.D., Anderson-Teixeira, K.J., 2015. Larger trees suffer most during drought in forests worldwide. Nat. Plants 1 (10), 1–5. https://doi.org/10.1038/NPLANTS.2015.139.

Bittencourt, P.R.L., Oliveira, R.S., Costa, A.C.L., Giles, A.L., Coughlin, I., Costa, P.B., et al., 2020. Amazonia trees have limited capacity to acclimate plant hydraulic

properties in response to long-term drought. Glob. Chang. Biol. 26 (6), 3569–3584. https://doi.org/10.1111/gcb.15040.

Britton, T.G., Brodribb, T.J., Richards, S.A., Ridley, C., Hovenden, M.J., 2022. Canopy damage during a natural drought depends on species identity, physiology and stand composition. New Phytol. 233 (5), 2058–2070. https://doi.org/10.1111/nph.17888.

Brodribb, T.J., Powers, J., Cochard, H., Choat, B., 2020. Hanging by a thread? Forests and drought. Science 368 (6488), 261–266. https://doi.org/10.1126/science.aat7631.

Brodribb, T.J., Holbrook, N.M., 2003. Stomatal closure during leaf dehydration, correlation with other leaf physiological traits. Plant Physiol. 132 (4), 2166–2173. https://doi.org/10.1104/pp.103.023879.

Bucci, S.J., Scholz, F.G., Peschiutta, M.L., Arias, N.S., Meinzer, F.C., Goldstein, G., 2013. The stem xylem of Patagonian shrubs operates far from the point of catastrophic dysfunction and is additionally protected from drought-induced embolism by leaves and roots. Plant Cell Environ. 36 (12), 2163–2174. https://doi.org/10.1111/pce.12126.

Chen, Y.J., Cao, K.F., Schnitzer, S.A., Fan, Z.X., Zhang, J.L., Bongers, F., 2015. Water-use advantage for lianas over trees in tropical seasonal forests. New Phytol. 205 (1), 128–136. https://doi.org/10.1111/nph.13036.

Chen, Y.J., Choat, B., Sterck, F., Maenpuen, P., Katabuchi, M., Zhang, S.B., et al., 2021a. Hydraulic prediction of drought-induced plant dieback and top-kill depends on leaf habit and growth form. Ecol. Lett. 24 (11), 2350–2363. https://doi.org/10.1111/ele.13856.

Chen, Y.J., Maenpuen, P., Zhang, Y.J., Barai, K., Katabuchi, M., Gao, H., et al., 2021b. Quantifying vulnerability to embolism in tropical trees and lianas using five methods: can discrepancies be explained by xylem structural traits? New Phytol. 229 (2), 805–819. https://doi.org/10.1111/nph.16927.

Chitra Tarak, R., Xu, C., Aguilar, S., Anderson Teixeira, K.J., Chambers, J., Detto, M., et al., 2021. Hydraulically-vulnerable trees survive on deep-water access during droughts in a tropical forest. New Phytol. 231 (5), 1798–1813. https://doi.org/10.1111/nph.17464.

Choat, B., Brodribb, T.J., Brodersen, C.R., Duursma, R.A., López, R., Medlyn, B.E., 2018. Triggers of tree mortality under drought. Nature 558 (7711), 531–539. https://doi.org/10.1038/s41586-018-0240-x.

Choat, B., Jansen, S., Brodribb, T.J., Cochard, H., Delzon, S., Bhaskar, R., et al., 2012. Global convergence in the vulnerability of forests to drought. Nature 491 (7426), 752–755. https://doi.org/10.1038/nature11688.

Cook, B.I., Smerdon, J.E., Seager, R., Coats, S., 2014. Global warming and 21st century drying. Clim. Dyn. 43 (9–10), 2607–2627. https://doi.org/10.1007/s00382-014-2075-y.

Creek, D., Blackman, C.J., Brodribb, T.J., Choat, B., Tissue, D.T., 2018. Coordination between leaf, stem, and root hydraulics and gas exchange in three arid-zone angiosperms during severe drought and recovery. Plant Cell Environ. 41 (12), 2869–2881. https://doi.org/10.1111/pce.13418.

Creek, D., Lamarque, L.J., Torres-Ruiz, J.M., Parise, C., Delzon, S., 2019. Xylem embolism in leaves does not occur with open stomata: evidence from direct observations using the optical visualisation technique. J. Exp. Bot. 71 (3), 1151–1159. https://doi.org/10.1093/jxb/erz474.

Dahlin, K.M., Ponte, D.D., Setlock, E., Nagelkirk, R., 2017. Global patterns of drought deciduous phenology in semi-arid and savanna-type ecosystems. Ecography 40 (2), 314–323. https://doi.org/10.1111/ecog.02443.

Dai, A., 2013. Increasing drought under global warming in observations and models. Nat. Clim. Chang. 3 (1), 52–58. https://doi.org/10.1038/nclimate1633.

Delzon, S., Cochard, H., 2014. Recent advances in tree hydraulics highlight the ecological significance of the hydraulic safety margin. New Phytol. 203 (2), 355–358. https://doi.org/10.1111/nph.12798.

Duursma, R., Choat, B., 2017. fitplc - an R package to fit hydraulic vulnerability curves. J. Plant Hydraul. 4, 2. https://doi.org/10.20870/jph.2017.e002.

Ehrlén, J., Morris, W.F., 2015. Predicting changes in the distribution and abundance of species under environmental change. Ecol. Lett. 3 (18), 303–314. https://doi.org/10.1111/ele.12410.

Eller, C.B., Lima, A.L., Oliveira, R.S., 2016. Cloud forest trees with higher foliar water uptake capacity and anisohydric behavior are more vulnerable to drought and climate change. New Phytol. 211 (2), 489–501. https://doi.org/10.1111/nph.13952.

Enquist, B.J., Enquist, C.A.F., 2011. Long-term change within a Neotropical forest: assessing differential functional and floristic responses to disturbance and drought. Glob. Chang. Biol. 17 (3), 1408–1424. https://doi.org/10.1111/j.1365-2486.2010.02326.x.

Fettig, C.J., Mortenson, L.A., Bulaon, B.M., Foulk, P.B., 2019. Tree mortality following drought in the central and southern Sierra Nevada, California, U.S. For. Ecol. Manag. 432, 164–178. https://doi.org/10.1016/j.foreco.2018.09.006.

Fox, J., Weisberg, S., 2019. An R companion to Applied Regression. Sage, Thousand Oaks CA. URL: https://socialsciences.mcmaster.ca/jfox/Books/Companion/.

Fu, P., Jiang, Y., Wang, A., Brodribb, T.J., Zhang, J., Zhu, S., et al., 2012. Stem hydraulic traits and leaf water-stress tolerance are co-ordinated with the leaf phenology of angiosperm trees in an Asian tropical dry karst forest. Ann. Bot. 110 (1), 189–199. https://doi.org/10.1093/aob/mcs092.

Fu, P., Zhu, S., Zhang, J., Finnegan, P.M., Jiang, Y., Lin, H., et al., 2019. The contrasting leaf functional traits between a karst forest and a nearby non-karst forest in south-west China. Funct. Plant Biol. 46 (10), 907. https://doi.org/10.1071/FP19103.

Geekiyanage, N., Goodale, U.M., Cao, K., Kitajima, K., 2019. Plant ecology of tropical and subtropical karst ecosystems. Biotropica 51 (5), 626–640. https://doi.org/10.1111/btp.12696.

Gutierrez Lopez, J., Tor Ngern, P., Oren, R., Kozii, N., Laudon, H., Hasselquist, N.J., 2021. How tree species, tree size, and topographical location influenced tree

transpiration in northern boreal forests during the historic 2018 drought. Glob. Chang. Biol. 27 (13), 3066–3078. https://doi.org/10.1111/gcb.15601.

Hammond, W.M., Yu, K., Wilson, L.A., Will, R.E., Anderegg, W.R.L., Adams, H.D., 2019. Dead or dying? Quantifying the point of no return from hydraulic failure in drought-induced tree mortality. New Phytol. 223 (4), 1834–1843. https://doi.org/10.1111/nph.15922.

Harrell, F.E. Jr., 2022. Hmisc: Harrell miscellaneous. URL: https://CRAN.R-project.org/package=Hmisc.

He, P., Lian, J., Ye, Q., Liu, H., Zheng, Y., Yu, K., et al., 2022. How do functional traits influence tree demographic properties in a subtropical monsoon forest? Funct. Ecol. https://doi.org/10.1111/1365-2435.14189. Online Version of Record.

Iverson, L.R., Prasad, A.M., 1998. Predicting abundance of 80 tree species following climate change in the Eastern United States. Ecol. Monogr. 68 (4), 465–485. https://doi.org/10.1890/0012-9615(1998)068[0465:PAOTSF]2.0.CO;2.

Johnson, D.M., Berry, Z.C., Baker, K.V., Smith, D.D., Mcculloh, K.A., Domec, J.C., 2018. Leaf hydraulic parameters are more plastic in species that experience a wider range of leaf water potentials. Funct. Ecol. 32 (4), 894–903. https://doi.org/10.1111/1365-2435.13049.

Klein, T., Niu, S., Niu, S., 2014. variability of stomatal sensitivity to leaf water potential across tree species indicates a continuum between isohydric and anisohydric behaviours. Funct. Ecol. 28 (6), 1313–1320. https://doi.org/10.1111/1365-2435.12289.

Levionnois, S., Ziegler, C., Heuret, P., Jansen, S., Stahl, C., Calvet, E., et al., 2021. Is vulnerability segmentation at the leaf-stem transition a drought resistance mechanism? A theoretical test with a trait-based model for Neotropical canopy tree species. Ann. For. Sci. 78 (4) https://doi.org/10.1007/s13595-021-01094-9.

Levionnois, S., Ziegler, C., Jansen, S., Calvet, E., Coste, S., Stahl, C., et al., 2020. Vulnerability and hydraulic segmentations at the stem-leaf transition: coordination across Neotropical trees. New Phytol. 228 (2), 512–524. https://doi.org/10.1111/nph.16723.

Li, R., Zhu, S., Chen, H.Y.H., John, R., Zhou, G., Zhang, D., et al., 2015. Are functional traits a good predictor of global change impacts on tree species abundance dynamics in a subtropical forest? Ecol. Lett. 18 (11), 1181–1189. https://doi.org/10.1111/ele.12497.

Li, S.F., Valdes, P.J., Farnsworth, A., Davies-Barnard, T., Zhou, Z.K., 2021. Orographic evolution of northern Tibet shaped vegetation and plant diversity in eastern Asia. Sci. Adv. 7 (5), c7741. https://doi.org/10.1126/sciadv.abc774.

Liu, W., Li, P., Duan, W., Liu, W., 2014. Dry-season water utilization by trees growing on thin karst soils in a seasonal tropical rainforest of Xishuangbanna, Southwest China. Ecohydrology 7 (3), 927–935. https://doi.org/10.1002/eco.1419.

Liu, Y., Song, J., Wang, M., Li, N., Niu, C., Hao, G., 2015. Coordination of xylem hydraulics and stomatal regulation in keeping the integrity of xylem water transport in shoots of two compound-leaved tree species. Tree Physiol. 35 (12), 1333–1342. https://doi.org/10.1093/treephys/tpv061.

Liu, Y., Yoon, S., Kim, J., Xiong, L., Lee, J., 2021. Changes in intensity and variability of tropical cyclones over the Western North Pacific and their local impacts under different types of El Niños. Atmosphere 12 (1), 59. https://doi.org/10.3390/atmos12010059.

Martínez-Garza, C., Tobon, W., Campo, J., Howe, H.F., 2013. Drought mortality of tree seedlings in an eroded tropical pasture. Land Degrad. Dev. 24 (3), 287–295. https://doi.org/10.1002/ldr.1127.

Mcculloh, K.A., Johnson, D.M., Petitmermet, J., Mcnellis, B., Meinzer, F.C., Lachenbruch, B., 2015. A comparison of hydraulic architecture in three similarly sized woody species differing in their maximum potential height. Tree Physiol. 35 (7), 723–731. https://doi.org/10.1093/treephys/tpv035.

McDowell, N.G., 2011. Mechanisms linking drought, hydraulics, carbon metabolism, and vegetation mortality. Plant Physiol. 155 (3), 1051–1059. https://doi.org/10.1104/pp.110.170704.

Meinzer, F.C., Johnson, D.M., Lachenbruch, B., Mcculloh, K.A., Woodruff, D.R., 2009. Xylem hydraulic safety margins in woody plants: coordination of stomatal control of xylem tension with hydraulic capacitance. Funct. Ecol. 23 (5), 922–930. https://doi.org/10.1111/j.1365-2435.2009.01577.x.

Meir, P., Mencuccini, M., Dewar, R.C., 2015. Drought-related tree mortality: addressing the gaps in understanding and prediction. New Phytol. 207 (1), 28–33. https://doi.org/10.1111/nph.13382.

Myers, N., Mittermeier, R.A., Mittermeier, C.G., Da, F.G., Kent, J., 2000. Biodiversity hotspots for conservation priorities. Nature 403 (6772), 853–858. https://doi.org/10.1038/35002501.

Nolan, R.H., Gauthey, A., Losso, A., Medlyn, B.E., Smith, R., Chhajed, S.S., et al., 2021. Hydraulic failure and tree size linked with canopy die-back in eucalypt forest during extreme drought. New Phytol. 230 (4), 1354–1365. https://doi.org/10.1111/nph.17298.

Perez-Harguindeguy, N., Diaz, S., Garnier, E., Lavorel, S., Poorter, H., Jaureguiberry, P., et al., 2016. New handbook for standardised measurement of plant functional traits worldwide. Aust. J. Bot. 64 (7–8), 715–716. https://doi.org/10.1071/BT12225_CO.

Phillips, O.L., van der Heijden, G., Lewis, S.L., Lopez-Gonzalez, G., Aragao, L.E., Lloyd, J., et al., 2010. Drought-mortality relationships for tropical forests. New Phytol. 187 (3), 631–646. https://doi.org/10.1111/j.1469-8137.2010.03359.x.

Pivovaroff, A.L., Cook, V.M.W., Santiago, L.S., 2018. Stomatal behaviour and stem xylem traits are coordinated for woody plant species under exceptional drought conditions. Plant Cell Environ. 41 (12), 2617–2626. https://doi.org/10.1111/pce.13367.

Pivovaroff, A.L., Sack, L., Santiago, L.S., 2014. Coordination of stem and leaf hydraulic conductance in southern California shrubs: a test of the hydraulic segmentation hypothesis. New Phytol. 203 (3), 842–850. https://doi.org/10.1111/nph.12850.

Pivovaroff, A.L., Wolfe, B.T., McDowell, N., Christoffersen, B., Davies, S., Dickman, L.T., et al., 2021. Hydraulic architecture explains species moisture dependency but not

mortality rates across a tropical rainfall gradient. Biotropica 53 (4), 1213–1225. https://doi.org/10.1111/btp.12964.

Powers, J.S., Vargas, G.G., Brodribb, T.J., Schwartz, N.B., Pérez Aviles, D., Smith Martin, C.M., et al., 2020. A catastrophic tropical drought kills hydraulically vulnerable tree species. Glob. Chang. Biol. 26 (5), 3122–3133. https://doi.org/10.1111/gcb.15037.

Qiao, Y., Jiang, Y., Zhang, C., 2021. Contribution of karst ecological restoration engineering to vegetation greening in southwest China during recent decade. Ecol. Indic. 121, 107081 https://doi.org/10.1016/j.ecolind.2020.107081.

Qiu, J., 2010. China drought highlights future climate threats. Nature 465 (7295), 142–143. https://doi.org/10.1038/465142a.

Rowland, L., Da Costa, A.C.L., Galbraith, D.R., Oliveira, R.S., Binks, O.J., Oliveira, A.A. R., et al., 2015. Death from drought in tropical forests is triggered by hydraulics not carbon starvation. Nature 528 (7580), 119–122. https://doi.org/10.1038/nature15539.

Senf, C., Buras, A., Zang, C.S., Rammig, A., Seidl, R., 2020. Excess forest mortality is consistently linked to drought across Europe. Nat. Commun. 11 (1) https://doi.org/10.1038/s41467-020-19924-1.

Skelton, R.P., Brodribb, T.J., Mcadam, S., Mitchell, P.J., 2017. Gas exchange recovery following natural drought is rapid unless limited by loss of leaf hydraulic conductance: evidence from an evergreen woodland. New Phytol. 215 (4), 1399–1412. https://doi.org/10.1111/nph.14652.

Soudzilovskaia, N.A., Elumeeva, T.G., Onipchenko, V.G., Shidakov, I.I., Salpagarova, F. S., Khubiev, A.B., et al., 2013. Functional traits predict relationship between plant abundance dynamic and long-term climate warming. Proc. Natl. Acad. Sci. 110 (45), 18180–18184. https://doi.org/10.1073/pnas.1310700110.

Sperry, J.S., Donnelly, J.R., Tyree, M.T., 1988. A method for measuring hydraulic conductivity and embolism in xylem. Plant Cell Environ. 11 (1), 35–40. https://doi.org/10.1111/j.1365-3040.1988.tb01774.x.

Tan, F., Song, H., Fu, P., Chen, Y., Siddiq, Z., Cao, K., et al., 2020. Hydraulic safety margins of co-occurring woody plants in a tropical karst forest experiencing frequent extreme droughts. Agric. For. Meteorol. 292-293, 108107 https://doi.org/10.1016/j.agrformet.2020.108107.

Trugman, A.T., Detto, M., Bartlett, M.K., Medvigy, D., Anderegg, W.R.L., Schwalm, C., et al., 2018. Tree carbon allocation explains forest drought-kill and recovery patterns. Ecol. Lett. 21 (10), 1552–1560. https://doi.org/10.1111/ele.13136.

Tyree, M.T., Ewers, F.W., 1991. The hydraulic architecture of trees and other woody plants. New Phytol. 119 (3), 345–360. https://doi.org/10.1111/j.1469-8137.1991.tb00035.x.

Tyree, M.T., Hammel, H.T., 1972. The measurement of the turgor pressure and the water relations of plants by the pressure-bomb technique. J. Exp. Bot. 23 (1), 267–282. https://doi.org/10.1093/jxb/23.1.267.

Uriarte, M., Schwartz, N., Powers, J.S., Marín Spiotta, E., Liao, W., Werden, L.K., 2016. Impacts of climate variability on tree demography in second growth tropical forests: the importance of regional context for predicting successional trajectories. Biotropica 48 (6), 780–797. https://doi.org/10.1111/btp.12380.

Wang, Q., Zeng, J., Qi, J., Zhang, X., Zeng, Y., Shui, W., et al., 2021. A multi-scale daily SPEI dataset for drought characterization at observation stations over mainland China from 1961 to 2018. Earth Syst. Sci. Data 13 (2), 331–341. https://doi.org/10.5194/essd-13-331-2021.

Wheeler, J.K., Huggett, B.A., Tofte, A.N., Rockwell, F.E., Holbrook, N.M., 2013. Cutting xylem under tension or supersaturated with gas can generate PLC and the appearance of rapid recovery from embolism. Plant Cell Environ. 36 (11), 1938–1949. https://doi.org/10.1111/pce.12139.

Wickham, H., 2016. ggplot2: elegant graphics for data analysis. URL: 10.1007/978-3-319-24277-4.

Xia, S., Chen, J., Schaefer, D., Goodale, U.M., 2016. Effect of topography and litterfall input on fine-scale patch consistency of soil chemical properties in a tropical rainforest. Plant Soil 404 (1–2), 385–398. https://doi.org/10.1007/s11104-016-2854-9.

Zhang, S., Wen, G., Yang, D., 2019. Drought-induced mortality is related to hydraulic vulnerability segmentation of tree species in a Savanna ecosystem. Forests 10 (8), 697. https://doi.org/10.3390/f10080697.

Zhang, W., Zhao, J., Pan, F., Li, D., Chen, H., Wang, K., 2015. Changes in nitrogen and phosphorus limitation during secondary succession in a karst region in southwest China. Plant Soil 391 (1–2), 77–91. https://doi.org/10.1007/s11104-015-2406-8.

Zhang, X., Zwiers, F.W., Hegerl, G.C., Lambert, F.H., Gillett, N.P., Solomon, S., et al., 2007. Detection of human influence on twentieth-century precipitation trends. Nature 448 (7152), 461–465. https://doi.org/10.1038/nature06025.

Zhou, G., Houlton, B.Z., Wang, W., Huang, W., Xiao, Y., Zhang, Q., et al., 2014. Substantial reorganization of China's tropical and subtropical forests: based on the permanent plots. Glob. Chang. Biol. 20 (1), 240–250. https://doi.org/10.1111/gcb.12385.

Zhu, H., Wang, H., Li, B., Sirirugsa, P., 2003. Biogeography and floristic affinities of the limestone flora in Southern Yunnan, China. Ann. Mo. Bot. Gard. 90 (3), 444–465. https://doi.org/10.2307/3298536.

Zhu, S., Chen, Y., Fu, P., Cao, K., 2017. Different hydraulic traits of woody plants from tropical forests with contrasting soil water availability. Tree Physiol. 37 (11), 1469–1477. https://doi.org/10.1093/treephys/tpx094, 10.2307/3298536.

Zhu, X., Zou, X., Lu, E., Deng, Y., Luo, Y., Chen, H., et al., 2021. Litterfall biomass and nutrient cycling in karst and nearby non-karst forests in tropical China: a 10-year comparison. Sci. Total Environ. 758, 143619 https://doi.org/10.1016/j.scitotenv.2020.143619.

Ziegler, C., Coste, S., Stahl, C., Delzon, S., Levionnois, S., Cazal, J., et al., 2019. Large hydraulic safety margins protect Neotropical canopy rainforest tree species against hydraulic failure during drought. Ann. For. Sci. 76 (4) https://doi.org/10.1007/s13595-019-0905-0.